Controlled Particle Placement through Convective and Capillary Assembly

ARTICLE *in* LANGMUIR · DECEMBER 2007

Impact Factor: 4.46 · DOI: 10.1021/la700852c · Source: PubMed

Controlled Particle Placement through Convective and Capillary Assembly

Laurent Malaquin,† Tobias Kraus,‡ Heinz Schmid, Emmanuel Delamarche, and Heiko Wolf*

IBM Research GmbH, Zurich Research Laboratory, Säumerstrasse 4, 8803 Rüschlikon, Switzerland

Received March 23, 2007. In Final Form: July 3, 2007

A wide variety of methods are now available for the synthesis of colloidal particle having controlled shapes, structures, and dimensions. One of the main challenges in the development of devices that utilize micro- and nanoparticles is still particle placement and integration on surfaces. Required are engineering approaches to control the assembly of these building blocks at accurate positions and at high yield. Here, we investigate two complementary methods to create particle assemblies ranging from full layers to sparse arrays of single particles starting from colloidal suspensions of gold and polystyrene particles. *Convective assembly* was performed on hydrophilic substrates to create crystalline mono- or multilayers using the convective flow of nanoparticles induced by the evaporation of solvent at the three-phase contact line of a solution. On hydrophobic surfaces, *capillary assembly* was investigated to create sparse arrays and complex three-dimensional structures using capillary forces to trap and organize particles in the recessed regions of a template. In both methods, the hydrodynamic drag exerted on the particle in the suspension plays a key role in the assembly process. We demonstrate for the first time that the velocity and direction of particles in the suspension can be controlled to perform assembly or disassembly of particles. This is achieved by setting the temperature of the colloidal suspension above or below the dew point. The influence of other parameters, such as substrate velocity, wetting properties, and pattern geometry, is also investigated. For the particular case of capillary assembly, we propose a mechanism that takes into account the relative influences of these parameters on the motion of particles and that describes the influence of temperature on the assembly efficiency.

1. Introduction

Significant progress has been made in the synthesis of particles having well-defined compositions, shapes, structures and sizes.[1] Such particles have advantageous properties that render them suitable as potential building blocks for the fabrication of novel micro- and nanosystems.[2] Nevertheless, one of the main challenges in the development of devices that use micro- and nanoparticles is particle placement and integration on surfaces. Some of the most interesting properties appear only in well-ordered particle arrangements. For instance, organized colloidal arrays exhibit collective optical, magnetic, or transport properties[3] that enable novel optical devices,[4−7] highly sensitive chemical sensors,[8] or high-density data-storage applications.[9,10] Other applications rely on the specific properties that appear at the single-particle level or that arise from coupling between regularly spaced particles. These applications cover a large variety of fields, including electronics,[11] plasmonics,[12,13] and biology.[14]

Self-assembly can be defined as the autonomous organization of objects into ordered structures. It is one of the most efficient methods to order large numbers of small particles on surfaces. Self-assembly usually relies on the interaction forces between particles and/or particles and surfaces to drive the formation of ordered arrangements. The resulting structures, however, are often limited to certain dense packings, whereas the placement of individual objects through self-assembly remains difficult. Techniques combining self-assembly with chemical or topographical patterning of the substrate are well-suited to address this limitation. In the so-called directed assembly technique, patterning is used to create a well-defined spatial distribution of forces that direct the motion of particles toward specific areas of the substrate. Directed assembly has received constant interest throughout the years, and a wide variety of methods have been investigated.[4,15−18] Processes involving magnetic or electrostatic forces, sedimentation, physical confinement, or host−guest interactions have been reported.[19] Another set of approaches relies on capillary forces[20−22] and convective flows,[23−25] which are particularly well-suited for the assembly of particles in the

* Corresponding author. E-mail: hwo@zurich.ibm.com.

† Present address: Laboratoire Physicochimie−Curie, UMR/CNRS 168, Institut Curie, 26 rue d'Ulm, 75248 Paris, France.

‡ Also affiliated with the Laboratory for Surface Science and Technology, Department of Materials, ETH Zurich, Wolfgang-Pauli-Strasse 10, 8093 Zürich, Switzerland.

(1) Caruso, F. *Colloids and Colloidal Assemblies*; Wiley-VCH: Weinheim, Germany, 2004.
(2) Shipway, A. N.; Katz, E.; Willner, I. *ChemPhysChem* **2000**, *1*, 19.
(3) Pileni, M. P. *J. Phys. Chem. B* **2001**, *105*, 3358.
(4) Lopez, C. *Adv. Mater.* **2003**, *15*, 1679.
(5) Yang, S. M.; Miguez, H.; Ozin, G. A. *Adv. Funct. Mater.* **2002**, *12*, 425.
(6) Vlasov, Y. A.; Bo, X.-Z.; Sturm, J. C.; Norris, D. J. *Nature* **2001**, *414*, 289.
(7) Garcia-Santamaria, F.; Miyasaki, H. T.; Urquia, A.; Ibisate, M.; Belmonte, M.; Shinya, N.; Meseguer, F.; Lopez, C. *Adv. Mater.* **2002**, *14*, 1144.
(8) Holtz, J. H.; Asher, S. A. *Nature* **1997**, *389*, 829.
(9) Kobayashi, N.; Egami, C. *Opt. Lett.* **2005**, *30*, 209.
(10) Gourevich, I.; Pham, H.; Jonkman, J. E. N.; Kumacheva, E. *Chem. Mater.* **2004**, *16*, 1472.
(11) Amlani, I.; Rawlett, A. M.; Nagahara, L. A.; Tsui, R. K. *Appl. Phys. Lett.* **2002**, *80*, 2761.
(12) Maier, S. A.; Brongersma, M. L.; Kik, P. G.; Meltzer, S.; Requicha, A. A. G.; Atwater, H. A. *Adv. Mater.* **2001**, *13*, 1501.
(13) Hutter, E.; Fendler, J. H. *Adv. Mater.* **2004**, *16*, 1585.
(14) Steemer, F. J.; Ferguson, J. A.; Walt, D. R. *Nat. Biotech.* **2000**, *18*, 91.
(15) Xia, Y.; Gates, B.; Yin, Y.; Lu, Y. *Adv. Mater.* **2000**, *12*, 693.
(16) Norris, D. J.; Arlinghaus, E. G.; Meng, L.; Heiny, R.; Scriven, L. E. *Adv. Mater.* **2004**, *16*, 1393.
(17) Dziomkina, N.; Vancso, G. J. *Soft Matter* **2005**, *1*, 265.
(18) Roldughin, V. I. *Russ. Chem. Rev.* **2004**, *73*, 115.
(19) Mahalingam, V.; Onclin, S.; Péter, M.; Ravoo, B. J.; Huskens, J.; Reinhoudt, D. N. *Langmuir* **2004**, *20*, 11756.
(20) Cui, Y.; Björk, M. T.; Liddle, A.; Sönnichsen, C.; Boussert, B.; Alivisatos, A. P. *Nano Lett.* **2004**, *4*, 1093.
(21) Juillerat, F.; Solak, H. H.; Bowen, P.; Hofmann, H. *Nanotechnology* **2005**, *16*, 1311.
(22) Yin, Y.; Lu, Y.; Gates, B.; Xia, Y. *J. Am. Chem. Soc.* **2001**, *123*, 8718.
(23) Prevo, B. G.; Hwang, Y.; Velev, O. D. *Chem. Mater.* **2005**, *17*, 3642.
(24) Denkov, N. D.; Velev, O. D.; Kralchevsky, P. A.; Ivanov, I. B.; Yoshimura, H.; Nagayama, K. *Langmuir* **1992**, *8*, 3183.
(25) Denkov, N. D.; Velev, O. D.; Kralchevsky, P. A.; Ivanov, I. B.; Yoshimura, H.; Nagayama, K. *Nature* **1993**, *361*, 26.

10.1021/la700852c CCC: $37.00
Published on Web 10/02/2007

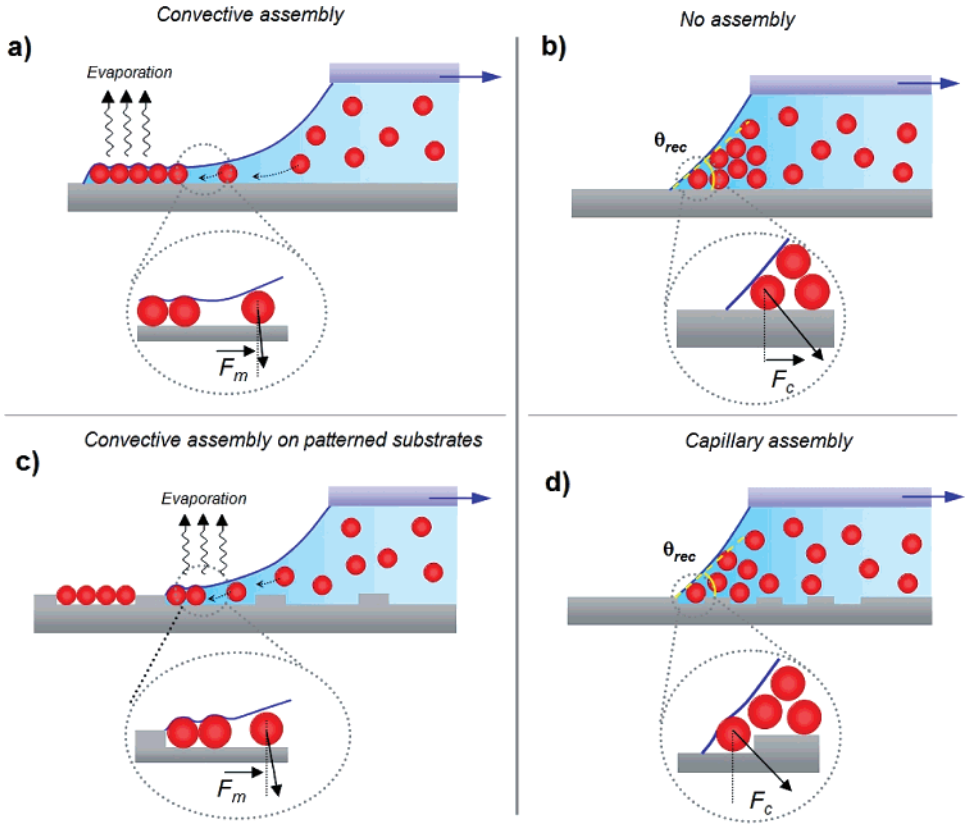

Figure 1. Various assembly mechanisms based on particle confinement at the contact line of a droplet can be distinguished depending on the wetting properties and topographical patterning of the substrate. Convective assembly is obtained on wetting substrates for contact angle values below 20°. The assembly mechanism is driven by the convective flow of solvent induced by evaporation at the contact line of the droplet, which leads, on flat surfaces, to the formation of continuous 2D layers of packed particles (a) or to 2D discontinuous arrangements on patterned surfaces (c). Capillary assembly takes place for receding contact angles θ_{rec} of the colloidal suspension greater than 20°. While no deposition occurs on flat surfaces (b), the combined effect of geometrical confinement and capillary forces created when the meniscus is pinned on the structures of a patterned substrate can be used to deposit only one or a few particles (d).

sub-micrometer regime. However, as these particles are usually provided as stable colloidal suspensions, these methods are applicable only if sedimentation remains negligible during the time frame of the assembly.

The work shown here covers two complementary mechanisms, namely, convective assembly[26] and capillary assembly, to create particle assemblies starting from colloidal suspension in water. Both are based on the confinement of particles induced at the three-phase contact line of a droplet that is dragged over a substrate.

Convective assembly is obtained on wetting substrates for contact angle values below ~20° (Figure 1a). The assembly mechanism is based on the convective flow of a solvent induced by evaporation of the droplet that drags the particles toward the contact line. The profile of the liquid meniscus close to the contact line leads to a vertical confinement of the suspended particles into a thin film of solvent. The assembly process starts when the thickness of the solvent layer becomes equal to the particle diameter.[25] The combined effects of convective flow and attractive capillary forces that arise when the top of the particles protrude from the solvent layer lead to the formation of extended layers or multilayers of closely packed particles.

We also investigated the combination of convective assembly with patterned substrates (Figure 1c). Using shallow patterns, this approach extends the range of structures achievable and allows for the creation of two-dimensional (2D) layers with controlled lattice parameters or discontinuous 2D structures.

When the contact angle of the liquid suspension increases, however, the confinement effect induced by the meniscus decreases. Above a critical contact angle value, the horizontal force exerted by the liquid meniscus becomes high enough to prevent particles from depositing onto a flat substrate (Figure 1b). In contrast, on patterned surfaces, the combined effects of capillary forces resulting from the local distortion of the meniscus when the contact line is dragged over the structures and the geometrical confinement induced by the structures lead to a selective immobilization of the particles in the recessed areas of the substrate, whereas no particles are deposited in the surrounding areas (Figure 1d). This capillary assembly mechanism is well suited for accurate placement of individual particles to create discontinuous one-dimensional (1D) or three-dimensional (3D) structures.

The aim of this work is to improve our understanding of the assembly mechanisms and extend their applicability to a wide range of structures and particle materials. We will show that controlling the hydrodynamic forces exerted on the suspended particles is critical for their immobilization and organization. The flows created by evaporation of the solvent predominate the mechanisms responsible for particle motion during the assembly. Adjusting the evaporation by means of the substrate temperature allows us to control both the yield and the speed of assembly and even to reverse the assembly process. The effect of parameters such as the surface tension, velocity of the substrate, pattern shape, and size was also investigated with respect to the yield and quality of the assembled structures. In addition, we propose a novel model that takes into account the influence

(26) Adachi, E.; Dimitrov, A. S.; Nagayama, K. *Langmuir* **1995**, *11*, 1057.

of these parameters on the motion of particles and elucidates the influence of temperature on the assembly process. We further show that precise control of the particle motion allows the range of achievable structures to be extended to almost any kind of particle arrangement, from single-particle arrays to complex 2D or 3D structures. Gold and polystyrene (PS) particles with diameters ranging from 100 to 500 nm were assembled on elastomer templates. In some cases, the assembled structures were further transferred by printing using a previously reported method.[27]

2. Experimental Section

Compounds. Aqueous dispersions of gold nanoparticles with a diameter of 100 nm (5.6×10^9 particles/mL) were purchased from British Biocell International, U.K. Aqueous dispersions of monodispersed PS particles (499 ± 5 nm, 1% of solid content) were purchased from Duke Scientific (Palo Alto, CA). The dispersion concentration was adjusted to values ranging from 0.1 to 5% of solid content by dilution with deionized water or by centrifugation (10 000 rpm, 5 min). We took advantage of the presence of surfactants in the dispersions to tune the wetting properties of the templates by appropriate dilution with deionized water. The exact composition of the continuous phase is unknown and considered proprietary by the provider.

Fabrication of Stamps and Masters. The assembly of nanoparticles was performed on poly(dimethylsiloxane) (PDMS) templates prepared by molding on flat or patterned silicon masters using the methods and materials reported in ref 28. The templates consist of an approximately 200-μm-thick PDMS layer on a 175-μm-thick glass backplane (D 263; Schott AG, Germany) derivatized with allyltrichlorosilane (ABCR). High-resolution masters were provided by AMO GmbH (Germany) and Xlith GmbH (Germany). They were fabricated by electron-beam lithography and reactive ion etching starting from silicon wafers and SOI (200 nm device layer thickness) wafers, respectively. The depth of the structures was 100 and 200 nm, respectively. The wafers were coated with an ~10-nm-thick anti-adhesive layer of $(CF_x)_y$ deposited from a C_4F_8/CF_4-based plasma (Multiplex ICP, STS, U.K.). After the PDMS was cured at 60 °C for 48 h, the samples were cut into square pieces of 1×1 cm^2. Prior to assembly, the templates were cleaned with ethanol and dried under a stream of nitrogen. Templates used for convective assembly were oxidized using an O_2 plasma treatment at 200 W for 20 s in a TePla 100-E reactor (Technics Plasma GmbH, Germany).

Experimental Setup. The setup used in this study is shown schematically in Figure 2. The PDMS templates were fixed on a motorized translation stage. A defined volume of solution (40 μL) was injected between the moving substrate and a slide fixed above the substrate at a distance of approximately 500 μm. The substrate was moved at velocities ranging from 0.05 to 200 μm s^{-1} with steps of 0.5 μm. To control the evaporation rate of the solution, a Peltier element was used to adjust the substrate temperature between 0 and 40 °C, with an accuracy of ±0.1 °C. The entire setup was mounted on the stage of an optical microscope to provide direct observation of the assembly process. A camera was also installed to allow in situ monitoring of the contact angle of the solution. Finally, a computer interface based on LabView (National Instruments, Austin, TX) was developed to control the temperature and substrate velocity during assembly. Image analysis and measurement of particle velocity were performed using particle-tracking software (Image Pro 5.0, Media Cybernetics).

Particle Transfer. The transfer of PS particles is described in ref 27. It was performed by bringing the processed templates into contact with a 2×2 cm^2 silicon piece (covered with native oxide) or a gold-coated (30−40 nm Au on Ti or Cr adhesion layer) silicon wafer piece placed on a hot plate and heated to 120 °C. The PDMS template was pressed slightly onto the substrate to promote conformal contact, which was monitored optically. Immediately after contact, template and substrate were removed from the hot plate, allowed to cool to room temperature, and finally separated.

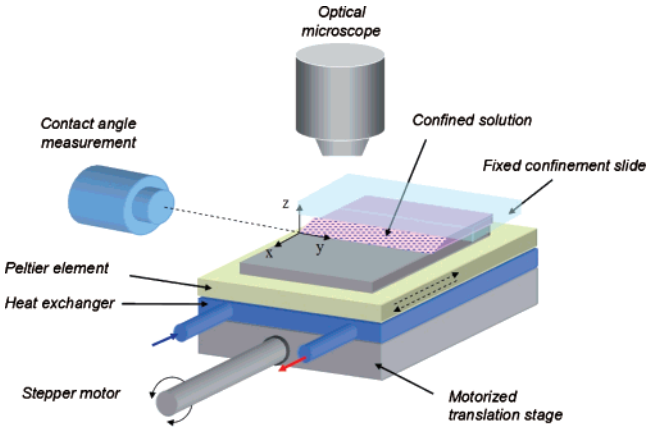

Figure 2. Illustration of the experimental setup developed for controlled convective and capillary assembly of particles on surfaces. The assembly is performed by dragging the liquid meniscus of a colloidal suspension droplet between a fixed slide and a moving substrate actuated by a stepper motor. The temperature of the substrate is controlled by a Peltier element.

3. Convective Assembly

The mechanism of convective assembly is described in refs 26, 29 and 30. The assembly is usually performed by dragging the meniscus of an aqueous colloidal suspension droplet over a hydrophilic surface at constant velocity. The growth of an ordered layer is caused by the convective transport of particles toward the already ordered array. A continuous flux of solvent from the thicker part of the layer compensates for water evaporation in the contact line area. This convective flow carries the suspended particles toward the contact line. The confinement effect induced by the meniscus coupled to the capillary forces appearing between particles during drying leads to the formation of a continuous 2D lattice. As the layer of particles grows, the substrate is withdrawn together with the already formed layer. If the withdrawal rate is equal to the rate of layer formation, a homogeneous layer grows continuously. For steady-state assembly, a simple equation describing the solvent flux and the accumulation of particles in the drying region was proposed by Dimitrov and Nagayama:[29]

$$v_c = \frac{\beta j_e l \phi}{h(1-\epsilon)(1-\phi)} \quad (1)$$

This equation establishes a relation between the growth velocity of the layer, v_c, the porosity, ϵ, the height of the assembled layer, h, the volume fraction ratio of the particles in the suspension, ϕ, a coefficient that relates the solvent velocity to the particle velocity, β ($0 < \beta < 1$), and the evaporation rate of pure water, j_e. The variable $l(x)$ is defined as $l = J_{evap}/j_e(x)$, where J_{evap} is the rate of evaporation averaged over the drying length, and $j_e(x)$ is the evaporation rate at any point of the drying region. This equation shows that three major process parameters can be used to control the coating thickness and structure: (i) the substrate velocity v_s, (ii) the particle volume fraction ϕ, and (iii) the solvent evaporation rate J_{evap}. At fixed evaporation rate and volume fraction, a uniform crystalline monolayer with a defined thickness is obtained if $v_c = v_s$ so that the nanoparticle influx toward the

(27) Kraus, T.; Malaquin, L.; Delamarche, E.; Schmid, H.; Spencer, N. D.; Wolf, H. *Adv. Mater.* **2005**, *17*, 2438.
(28) Geissler, M.; Wolf, H.; Stutz, R.; Delamarche, E.; Grummt, U. W.; Michel, B. *Langmuir* **2003**, *19*, 6301.
(29) Dimitrov, A. S.; Nagayama, K. *Langmuir* **1996**, *12*, 1303.
(30) Prevo, B. G.; Velev, O. D. *Langmuir* **2004**, *20*, 2099.

drying region exactly compensates for the particle consumption due to the layer growth. Increasing the substrate velocity above the natural assembly speed for a monolayer or, equivalently, decreasing the volume fraction of the suspension results in an incomplete layer. In contrast, decreasing the substrate velocity or increasing the volume fraction will result in the formation of multiple layers. Besides substrate velocity and volume fraction, the evaporation rate J_{evap} influences the growth velocity of the assembled layer according to eq 1. The evaporation rate depends on the temperature of the colloidal suspension and can therefore be controlled via the substrate temperature. The exact relationship is discussed in the next paragraphs.

Temperature Dependence. Attempts to influence the evaporation rate J_{evap} by modifying the relative humidity around the drying region were reported but led to differing conclusions.[30,24] Moreover, controlling the relative humidity is usually a slow process requiring a cumbersome experimental setup. The temperature dependence of the convective flows, in contrast, so far has not been studied. We will show that the adjustment of the substrate temperature T_s is an efficient way of controlling the evaporation rate $J_{evap} = f(T_s)$. We first investigated the influence of T_s on the formation of monolayers using suspensions of 500-nm-diameter PS particles in water. All experiments were carried out on freshly oxidized PDMS substrates. We recorded the evolution of the assembly rate in the temperature range $T_{dew} < T < 30$ °C, where T_{dew} is the dew point temperature. During the experiment, the substrate velocity v_s was adjusted until the position of the edge of the assembled layer remained stable relative to the observation field. This simple method ensured the creation of a uniform monolayer and provided an estimate of the growth rate of the monolayer v_c because, under the conditions chosen, $v_c \approx v_s$. Figure 3a shows a typical optical micrograph acquired during the assembly of 500-nm PS particles (0.2% solid content, $T_s = 18$ °C) on a flat PDMS substrate treated with oxygen plasma. The left-hand side of the image shows the assembled layer, whereas the right-hand side shows the liquid suspension of particles. Particles can be distinguished individually, and their position can be monitored and further analyzed.

Figure 3b shows the dependence of v_c on the surface temperature T_s for different solid contents ranging from 0.1 to 0.5%. In this experiment, the ambient temperature and relative humidity (RH) were 20 °C and 42%, respectively, and T_{dew} was 7.7 °C.

In accordance with previous studies,[29,30,31] we observed a large influence of the volume fraction ϕ on v_c. As eq 1 predicts, v_c increases with the concentration of the colloidal suspension. Independently of the solid content, v_c also increased nonlinearly with T_s. In the range of temperatures investigated, 10 °C $< T_s <$ 32 °C, the values of v_c obtained for $\phi = 0.5\%$ varied continuously from 10 μm s^{-1} at $T_s = 28$ °C to zero for temperatures close to T_{dew}. Decreasing ϕ to 0.1% limited the range of v_c to values between 0 and 1.5 μm s^{-1} at $T_s = 28$ °C. Because of the small volume of suspension required for our experiments (50 μL), the deposition process could not be sped up indefinitely by increasing T_s. Indeed, the investigation of temperatures higher than 30 °C remains difficult because the high evaporation rate leads to a rapid increase of the solid content in the colloidal suspension, which almost doubles after 1 h of experiments.

Whereas the modification of v_c via controlling the relative humidity was shown to be experimentally difficult,[30] our results show that controlling the substrate temperature T_s is an efficient way of controlling J_{evap}. In view of the development of convective assembly as a relevant coating technology, the control of v_c via the temperature offers several advantages. First, the values of v_c accessible by controlling T_s can be tuned accurately, independently of the volume fraction. Second, a simple experimental setup such as that developed for these studies allows an accurate and fast adjustment of T_s, which provides the flexibility required for the growth of crystal layers.

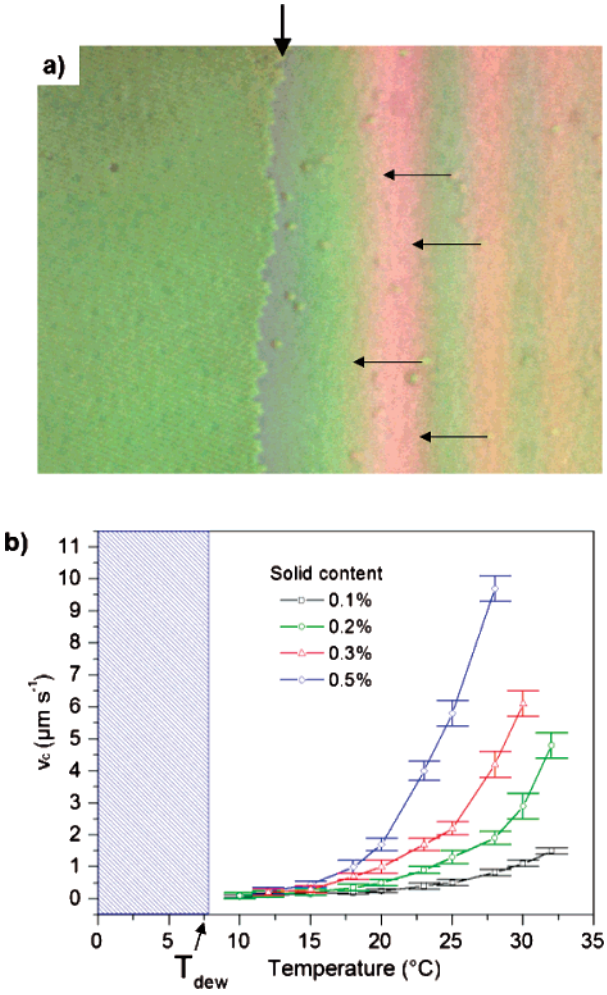

Figure 3. (a) Optical micrograph acquired during the convective assembly of 500-nm PS particles on a oxygen-plasma-treated PDMS substrate. Particles are dragged by the convective flow from the bulk liquid (right-hand side of the image) toward the contact line, where they are assembled into a continuous, densely packed monolayer (left-hand side of the image). (b) Depending on the temperature of the substrate T_s, the convective flow created by evaporation can be tuned to adjust the growth velocity v_c of the particle monolayer. The influence of T_s on v_c was investigated for various solid contents.

Reversibility of the Assembly Process. Careful investigations of the influence of the substrate temperature on particle motion were carried out for $T_s < T_{dew}$. Panels a, b, and c of Figure 4 show typical optical micrographs obtained during the assembly of 500 nm PS particles for $T_s > T_{dew}$, $T_s \approx T_{dew}$ and $T_s < T_{dew}$, respectively.

Above the dew point, the convective flow created by evaporation induces a particle influx toward the contact line (Figure 4a). Evaluation of the particle velocity close to the drying zone revealed a mean value $v = 19.8 \pm 0.8$ μm s^{-1} at $T =$ 20 °C and a substrate velocity of 0.5 μm s^{-1}.

Decreasing T_s resulted in the slowdown of the assembly. For $T_s \approx T_{dew}$, the evaporation of the solvent in the drying region was almost zero. As no particle flux was created, the assembly process stopped. This was confirmed by the analysis of the optical images recorded, which showed that the mean position of the particles

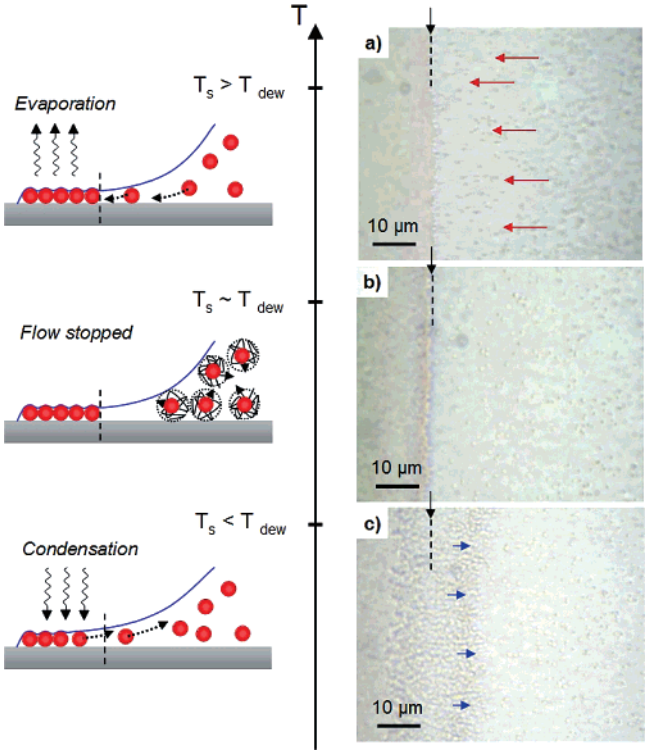

Figure 4. Illustration of the influence of the evaporation-induced convective flow on the assembly of 500-nm PS particles (0.2% solid content) on an oxygen-plasma-treated PDMS surface. For $T_s > T_{dew}$, the hydrodynamic force created by the flow drags particles to the contact line and leads to a monolayer formation (a). For $T_s \approx T_{dew}$, the evaporation of the solvent in the drying region is nearly zero (b). As no particle flux is created, the assembly process is stopped, and only the Brownian motion of particles is observable. For $T_s < T_{dew}$, condensation takes place on the already assembled layer and creates a reverse flow of solvent that disassembles the monolayer (c).

in the suspension was stable and that only Brownian motion of the particles remained (Figure 4b).

For T_s values below the dew point, condensation takes place in the former drying zone. A flow of water from the already assembled layer to the bulk liquid induces a progressive disintegration of the monolayer (Figure 4c). This disassembly mechanism is reversible, and layers can be disassembled and reassembled more than five times consecutively without adverse effects on the assembled lattices.

The accessibility of different regimes, namely, (i) assembly, (ii) stagnation, and (iii) disassembly, is a convenient feature of convective assembly. All these regimes can be accessed by adjusting the substrate temperature, which provides not only a very flexible way of initiating or inhibiting the assembly process but also the possibility to repair the assembled layers during their construction to eliminate defects such as voids or unintentional multilayer formation. Moreover, temperature control is a fast way of precisely controlling the assembly speed v_c and of decoupling it from ϕ and h.

Figure 5 shows examples of particle monolayers assembled from 500-nm PS (0.5% solid content; $\sim 7.3 \times 10^{10}$ particles/mL) and 100 nm Au ($\sim 5.6 \times 10^9$ particles/mL) particle suspensions. In both cases, the assembly was performed at a substrate temperature of 18 °C.

Because of their narrow size distribution (1.3% coefficient of variation), the assembly of PS particles gives rise to a dense, hexagonally packed monolayer (Figure 5a). Uniform layers with an area of up to 1 cm^2 were prepared. The assembled layers are polycrystalline with some defects such as vacancies or dislocations. While the quality of the layers is slightly better at lower v_c values, we could not observe a noticeable influence of the assembly velocity on the formation of dislocations and on the number of vacancies, which was estimated as 2.5×10^2 mm^{-2} (i.e., 100 ppm).

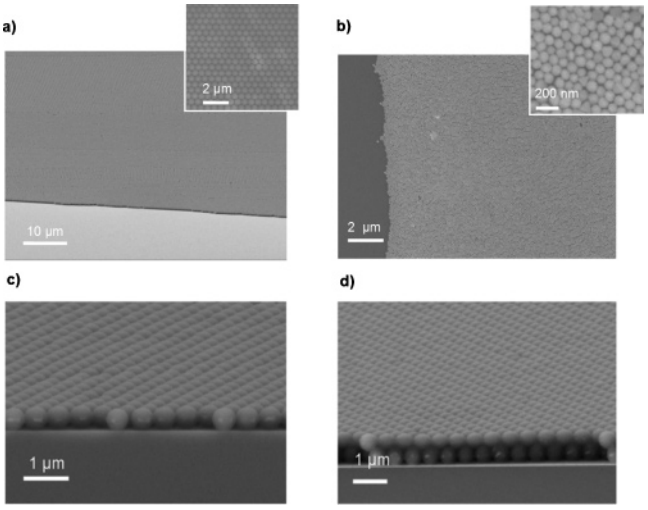

Figure 5. SEM images of 500-nm PS particles (a) and 100-nm gold nanoparticle monolayers (b) created by convective assembly on the surface of a flat PDMS substrate treated with oxygen plasma. Mono- (c) and bilayers (d) of PS particles were transferred in a single step onto a gold-coated silicon wafer heated to 120 °C.

Figure 5b shows an example of 100-nm Au particles assembled on the surface of an oxidized PDMS sample. This experiment was carried out at $T_s = 18$ °C, with a corresponding assembly rate of $v_c \approx 0.3$ μm s^{-1}. Uniform monolayers over a 5×5 mm^2 area were created at higher assembly rates. However, the variety of particle shapes usually encountered in gold particle suspensions was an obstacle for the fabrication of layers having large single-crystalline domains. We also observed that for $T_s > 25$ °C the stability of the monolayer growth was particularly sensitive to v_s, which had to be carefully tuned to v_c. For $v_s \geq 1$ μm s^{-1}, the condition $v_s = v_c$ is difficult to reach manually, and the assembly process is prone to rupture of the assembled layer or to accumulation of particles leading to multilayers. A decrease of T_s allows the assembly process to be slowed down to values of v_s below 1 μm s^{-1}, which offers better control of the monolayer fabrication.

Control of Multiple Layers Growth. Because of the implications the film thickness has, for the structural, optical, or electrical properties of the assembled structures, the influence of the different process parameters on the number of layers assembled has attracted much interest.[23,31,32] Usually, control is achieved by tuning the solid content or the velocity of the substrate. We found that controlling the assembly speed by means of the temperature provides more flexibility to create uniform multilayers with precisely controlled thickness. According to eq 1, a strong dependence of the layer thickness h on (i) the particle concentration, (ii) the inverse of the substrate velocity, and (iii) the local evaporation rate j_e is expected. The transition from monolayer to multilayer growth with a constant flux j_e should result in a significant slowdown of the assembly process. This hypothesis was confirmed by the work performed by Fustin et al. for particle suspensions having a solid content below 1%.[31]

(31) Fustin, C. A.; Glasser, G.; Spiess, H. W.; Jonas, U. *Langmuir* **2004**, *20*, 9114.
(32) Jiang, P.; Bertone, J. F.; Hwang, K. S.; Colvin, V. L. *Chem. Mater.* **1999**, *11*, 2132.

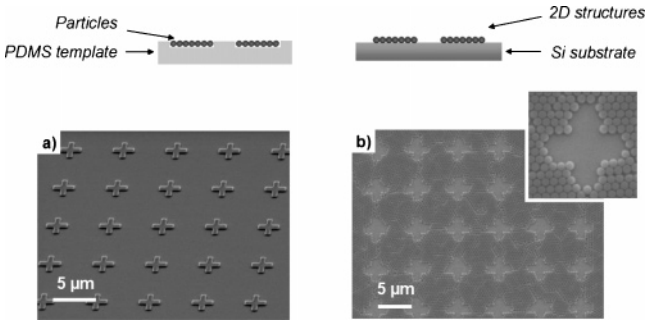

Figure 6. SEM image of a 2D arrangement of 500-nm PS particles created by convective assembly on a 200-nm-deep patterned PDMS substrate (a). This arrangement was transferred by printing on the surface of a gold-coated silicon wafer heated to 120 °C (b).

We observed that controlling the temperature allows one to compensate for the decrease of the assembly speed occurring while switching from monolayer to multilayer growth. Figure 5c,d shows side-view images of a single layer and a bilayer prepared from a 500-nm PS particle suspension (0.2% solid content). The structures were first assembled on a flat PDMS substrate and then transferred onto a Si wafer by printing. In this experiment, the substrate velocity was fixed to 0.6 μm s^{-1}, while the substrate temperature was used to modify the particle flux toward the contact line. A substrate temperature of $T_s = 20$ °C gave rise to stable monolayer formation, whereas increasing the temperature to $T_s = 26.5$ °C led to the creation of a bilayer. The number of layers N was monitored through optical observation of the deposited film. Because of interference between the light reflected from the top and bottom interfaces, a change in the layer thickness induces an abrupt color change that can be detected optically.

Templated Convective Assembly. The combination of convective assembly with templated surfaces has already been reported.[5,31,33] Two different approaches have been proposed, based either on chemical templates with hydrophobic−hydrophilic contrast or on topographical patterns. Both approaches are usually limited to continuous structures, such as opal microchannels or stripes of colloidal crystals oriented parallel to the convective flow. Structures oriented perpendicular to the convective flow act as obstacles for the motion of particles toward the drying region. We were able to demonstrate, however, that the use of very shallow patterns preserves the convective assembly mechanism and enables the fabrication of more complex structures. Such patterns do not affect the motion of particles toward the drying region until the thickness of the water film becomes less than the sum of the particle size and pattern height. When this condition is fulfilled, the protruding structures act as barriers for the motion of particles while a convective flow still takes place around these structures in the recessed area of the template. In these regions, the convective assembly mechanism is preserved and allows the selective assembly of particles into 2D structures.

Figure 6 shows an example of structures achieved on PDMS substrate with 200-nm-deep patterns using a colloidal suspension of 500-nm PS particles (0.1% solid content, $T_s = 20$ °C). The withdrawal velocity was set to 1.5 μm s^{-1}. After the assembly, the structures were transferred via printing. The presence of multiple dislocations in the structures can be explained by the mismatch between pattern size and integral multiples of the particle diameter.

(33) Yang, S. M.; Ozin, G. A. *Chem. Commun.* **2000**, *24*, 2507.

4. Capillary Assembly

On hydrophilic surfaces, the meniscus profile induces a vertical confinement of the particles close to the contact line that leads to the formation of ordered 2D continuous structures. On more hydrophobic surfaces, however, the component of the force exerted by the meniscus that is parallel to the substrate increases and becomes sufficiently strong to prevent particle deposition on flat surfaces. If the surface is patterned appropriately, this force component can be countered by a vertical structure. While the contact line is being dragged over the patterned substrate, the liquid meniscus is pinned and deforms around the structure. The combination of geometrical trapping at the substrate features and capillary forces exerted during film breakage leads to one particle or a small number of particles being confined close to the obstacle. As a result, particles are selectively trapped at the step edges of the template features, whereas no deposition occurs in the surrounding areas.

Nevertheless, the mechanism leading to particle deposition is not yet fully understood, particularly at the instance when the film breaks up over the structures. It is generally believed that the capillary forces created by the meniscus can overcome the thermal fluctuations as well as the other repulsive forces exerted on the particles and that they are responsible for the final deposition of particles on the surface.[20,22] Our experiments suggest that these capillary forces are important for, but not sufficient to explain particle trapping.

Influence of Temperature. As observable in convective assembly, the evaporation of the suspension deposited on a hydrophilic surface creates a flow of water that drags particles to the three-phase contact line. This mechanism was also observed for suspensions with contact angles between 20 and 60°. On such surfaces, it leads to an increase in the local density of particles close to the contact line. Our experiments suggest that the resulting accumulation region is essential to trigger the assembly process. Figure 7a,b shows two optical microscopy images taken during the assembly of 500-nm PS nanoparticles for two different substrate temperatures, $T_s = 27$ °C and $T_s = 32$ °C, respectively. This experiment was carried out on the surface of a patterned PDMS substrate with a colloidal suspension of 0.1% solid content. The patterns consisted of an array of crosses with a height of 200 nm. The measured ambient RH was 40%, and the dew point was estimated as 7 °C. In both experiments, we measured a receding contact angle of the colloidal suspension on the PDMS surface of 53 ± 2°.

The left part of the image (region I) shows the surface of the patterned substrate, whereas the right part of the image (region II) corresponds to the liquid suspension of particles. In the experiment performed at 27 °C, in situ observations did not show any particle immobilization on the substrate. This result was confirmed by scanning electron microscopy (SEM). When increasing the temperature to 32 °C, particles were selectively trapped in the structures as shown in Figure 7b with a yield of 99%. In addition to the immobilization of particles, the optical micrographs acquired during the assembly show a bright region close to the contact line (region III). While the exact determination of the solid content in this region is difficult, optical observations suggest a very close packing of the nanoparticles. Careful analysis of this accumulation region even revealed the presence of domains with different iridescent properties, suggesting that particles are ordered into polycrystalline arrangements.[34]

Our experiments imply that the creation of an accumulation zone is necessary to initiate the assembly process. We think that

(34) Russel, W. B.; Saville, D. A.; Schowalter, W. R. *Colloidal Dispersions*; Cambridge University Press: Cambridge, U.K., 1989.

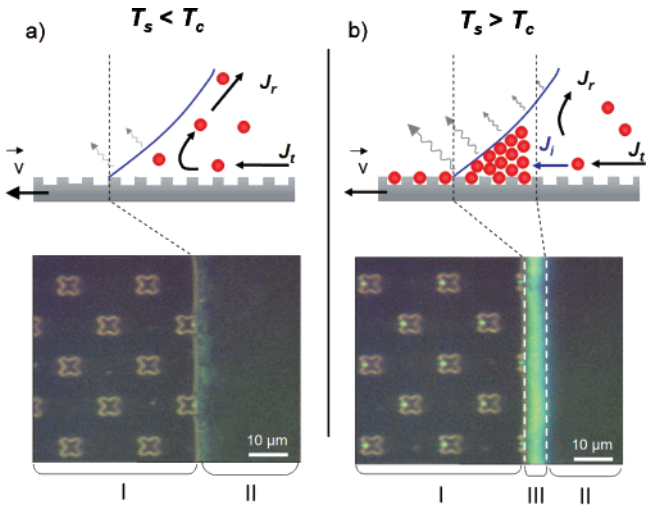

Figure 7. Illustration of the influence of temperature on the motion of particles during capillary assembly. The movement of the meniscus relative to the substrate induces a recirculation flow J_r that drags particles from the contact line region to the bulk liquid (Region II). (a) At low temperatures, evaporation does not compensate for the recirculation flow, and no particle deposition is observed (Region I). (b) As the substrate temperature T_s increases above the dew point, evaporation induces a particle flow J_i toward the contact line. This flow compensates for J_r and induces the accumulation of particles in Region III, which allows particle deposition into the substrate patterns (bright spots visible in the optical micrograph). The transition between the two mechanisms occurs at a substrate temperature T_c, where $J_t \approx J_r$. In this experiment, the assembly was performed at a constant substrate velocity $v_s = 1\ \mu m\ s^{-1}$ with a 0.1% solid content colloidal suspension.

the accumulation process assists the confinement of the particles in the structures in two ways. First, the local increase of the particle concentration due to their accumulation close to the contact line helps to increase the probability of trapping one particle in a structure. Second, the accumulation of particles close to the contact line contributes to the reduction of the mobility and fluctuations of particles in the substrate features shortly before the liquid breakup and further increases the trapping efficiency. The Brownian motion of a particle in a concentrated suspension is strongly reduced by the combined effects of the direct-interaction forces (Coulombic, van der Waals, etc.) and the hydrodynamic interactions between one particle and its neighbors. It has been demonstrated that the self-diffusion coefficient D_s, which characterizes particle mobility, is strongly sensitive to the volume fraction of particles in the suspension.[34] The reduction of particle mobility is visible in the accumulation region, where it causes optical effects such as iridescence, which indicates an ordered distribution of particles.[35,36]

The solvent flow responsible for particle accumulation is mainly induced by the evaporation of the solution and thus can be tuned by appropriate control of the substrate temperature. The relationship between T_s and particle motion is illustrated in Figure 7. At a temperature close to the dew point, the evaporation rate of the solution is almost zero. As the contact line is dragged over the substrate, a recirculation flow is induced in the liquid by the no-slip condition at the fixed wall. Because of Stokes drag, this flow induces a recirculation of particles J_r, as described in Figure 7a. When the temperature is increased above the dew point, an additional particle flow J_i toward the contact line is created by

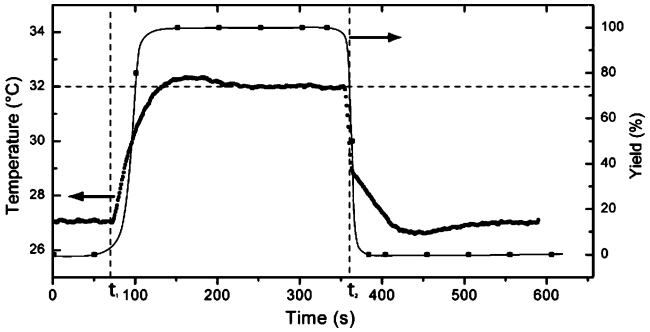

Figure 8. Temperature and time dependence of the capillary assembly yield of 500-nm PS particles on a PDMS template patterned with 200-nm-deep cross-shaped structures (see Figure 7). The assembly was performed at a constant substrate velocity $v_s = 1\ \mu m\ s^{-1}$ with a 0.1% solid content colloidal suspension. The receding contact angle of the colloidal suspension measured during the assembly was 44°.

solvent evaporation (Figure 7b). The total incoming particle flow is $J_t = J_i + J_r$. To start the accumulation process close to the contact line, J_i has to compensate for two phenomena: (i) the depletion of the accumulation zone due to recirculation and diffusion of particles from region III to the bulk liquid, and (ii) the particle loss due to deposition. Experimentally, this condition can be fulfilled by increasing the substrate temperature to a threshold value that we will call T_c.

As a validation of this model, we investigated the influence of T_s on the assembly yield of 500-nm PS particles (0.1% solid content) on a patterned PDMS substrate. Experiments were carried out with a constant substrate velocity of $1\ \mu m\ s^{-1}$. The influence of the evaporation rate was studied by switching the substrate temperature between 27 and 32 °C. The assembly yield was measured by subsequent analysis of image sequences taken during the experiment. Figure 8 shows the evolution of the temperature and assembly yield versus time during one cycle.

At $T_s = 27$ °C, no particle accumulation and immobilization could be observed. At t_1, the temperature setpoint was set to 32 °C. Optical observations revealed a transient period associated with an increase in the yield that first reached a value close to 80% for a substrate temperature of 30 °C and finally reached 99% at 32 °C. Temperature was then kept constant for 200 s. During this period, optical observations revealed a particle flux that lead to an increase in the particle concentration close to the contact line. The size of region III slowly increased during the experiment, indicating a progressive accumulation of particles. The image shown in Figure 7b (taken at $t = 250$ s) illustrates this mechanism. At $t = 360$ s, the temperature setpoint was set back to 27 °C. Within 20 s, the assembly yield dropped to 0%. Simultaneously, we observed a rapid depletion of region III, which finally led to a situation similar to the one depicted at $t = 0$ s (Figure 7a).

The existence of a temperature threshold T_c confirms the importance of the hydrodynamic flows created by evaporation on the assembly. This threshold corresponds to a situation in which the particle influx induced by evaporation overcomes the depletion due to diffusion, recirculation, and the deposition of particles on the surface. Control of the substrate temperature directly affects the balance between J_i and J_r, and therefore is an effective way of controlling the accumulation of particles and, thus, switching the assembly process on and off.

According to the above model, T_c is influenced by both the solid content of the colloidal dispersion and the substrate velocity responsible for the recirculation flow. Both dependencies are illustrated in Figure 9. The data show the evolution of T_c for the

(35) Dosho, S.; Ise, N.; Ito, K.; Iwai, S.; Kitano, H.; Matsuoka, H.; Nakamura, H.; Okumura, H.; Ono, T.; Sogami, I. S.; Ueno, Y.; Yoshida, H.; Yoshiyama, T. *Langmuir* **2000**, *2*, 394.
(36) Ise, N.; Matsuoka, H.; Ito, K.; Yoshida, H.; Yamanaka, J. *Langmuir* **2000**, *2*, 296.

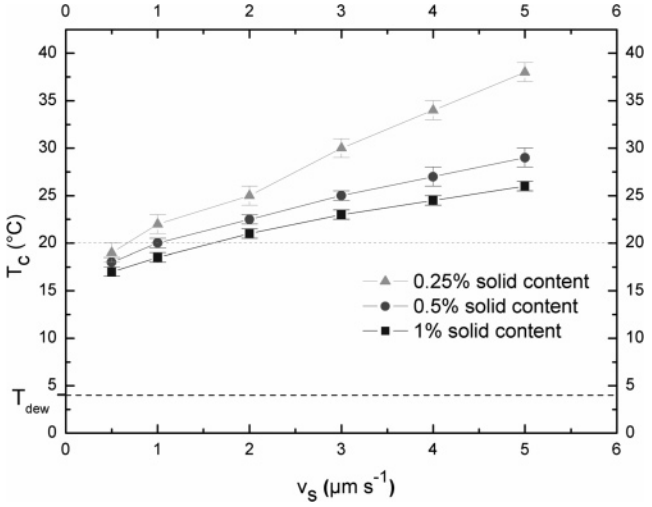

Figure 9. Evolution of the substrate temperature threshold T_c required to initiate the capillary assembly of 500-nm PS particles depending on the substrate velocity v_s and the particle solid content ϕ.

assembly of 500-nm PS particles on PDMS templates, which are similar to the one described in Figure 7. For this graph, T_c was defined as the minimum temperature leading to an assembly yield higher than 98%. The solid content of the dispersion was adjusted between 0.25 and 1%, whereas the concentration of the solutes in the continuous phase was adjusted to 25% of the original concentration by appropriate dilution and centrifugation steps. The substrate velocity was varied from 0.5 to 5 μm s^{-1}. As expected, T_c increases with the substrate velocity. When the velocity of the recirculation flow increases, the evaporation rate has to be raised to prevent depletion of region III. An increase of the solid content, on the other hand, allows one to reduce the temperature threshold. At a given temperature, the particle influx is nearly proportional to the solid content.

Influence of Surfactant Concentration. The major role of capillary forces renders the assembly process very sensitive to both the wetting properties of the colloidal suspension and the dimensions and shape of the structures. We first investigated the influence of the surface tension on the yield of the assembly process. Experiments were carried out by adjusting surfactant concentration while maintaining a constant particle solid content by appropriate dilution with deionized water and centrifugation steps. Contact angles were measured at a constant substrate velocity of 1 μm s^{-1}. Note that, for a given sample and surfactant concentration, we did not observe any significant influence of the velocity on the contact angle in the 0.5−5 μm s^{-1} range.

We found that there exists an optimum contact angle to trigger the assembly process. In the case of a colloidal suspension of 500-nm PS particles, this contact angle threshold value was found to be around 60 ± 4°. Above this value, no deposition could be observed, even if an accumulation region was established close to the contact line. Particle assembly was achieved for contact angle values between 30 and 60°. In this range, the vertical component of capillary forces appears to be sufficiently large to immobilize the particles, even in shallow patterns. Figure 10a,c shows arrays of crosses and squares with side lengths of 5 μm and a height of 200 nm, formed on PDMS substrates. PS particles (500 nm diameter) were assembled into arrays and lines with those structures. In both cases, the assembly was performed at 25 °C from a 0.2% solid content suspension. The contact angle was 50 ± 2°. The assembly yield was estimated to be 96%. Spaced arrays of 100-nm-wide gold nanoparticles were also obtained using 80-nm-deep and 120-nm-wide patterns on a PDMS template. The assembly was performed at a substrate temperature

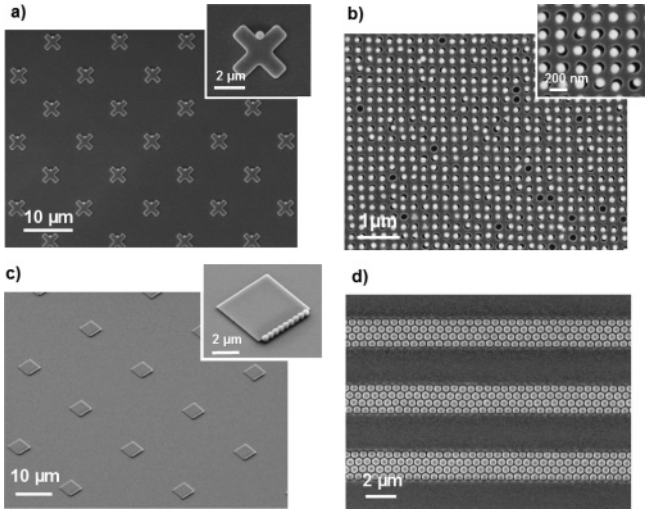

Figure 10. SEM images of spaced arrays and lines of 500-nm PS particles created by capillary assembly on 200-nm-deep patterned PDMS templates (a,c). In both cases, the assembly was performed at a substrate temperature $T_s = 25$ °C and a velocity $v_s = 1$ μm s^{-1} with a 0.2% solid content suspension (obtained by dilution of the initial suspension). Sparse arrays of 100-nm gold nanoparticles were obtained using 80-nm-deep and 120-nm-wide patterns on a PDMS template (b). PS particles (500 nm) were also assembled into 500-nm-deep and 1.7-μm-wide microchannels in PDMS (d). In the latter case, the assembly was performed at a substrate temperature $T_s =$ 29 °C and a substrate velocity $v_s = 0.75$ μm s^{-1} with a 0.3% solid content suspension.

of 28 °C and a substrate velocity of 0.2 μm s^{-1} (Figure 10b). For the gold particles, we found a threshold contact angle of approximately 50° for triggering the assembly. The formation of an accumulation region close to the contact line was also necessary to initiate the assembly, and a temperature threshold of approximately 25 °C was observed.

In general, increasing the surfactant concentration resulted in a decrease in the contact angle, which eventually led to a change from capillary to convective assembly for contact angle values of less than 15°. At this contact angle, the horizontal component of the capillary forces exerted by the meniscus becomes too weak to prevent particle deposition. As a consequence, a convective flow is created at the contact line, which leads to the assembly of nanoparticles into 2D layers.

Influence of Pattern Geometry and Orientation. Similar changes in assembly mechanism can occur as a result of the local contact line pinning induced by the substrate features. In the example shown in Figure 10d, 500-nm PS nanoparticles were assembled into 500-nm-deep and 1.7-μm-wide lines on a PDMS substrate. In these experiments, the withdrawal speed was varied between 1 and 10 μm s^{-1}. Because of the capillary pressure, the structures behaved as microfluidic channels and were filled by the colloidal dispersion, similar to the behavior of colloidal suspensions in closed microchannels.[37] Observation of the particle motion revealed that the assembly mechanism in the channel was close to convective assembly. The evaporation of the solvent created a flux of particles into the channels, and the lateral and vertical confinement led to the formation of closely packed 2D arrangements.

The magnitude and the direction of the capillary forces induced by the contact-line pinning depend strongly on the geometry of patterns. The influence of the pattern orientation on assembly yield and positions is illustrated in Figure 11, which shows three SEM images of particles assembled in 200-nm-deep cross-shaped

(37) Kim, E.; Xia, Y.; Whitesides, G. *Adv. Mater.* **1996**, *3*, 245.

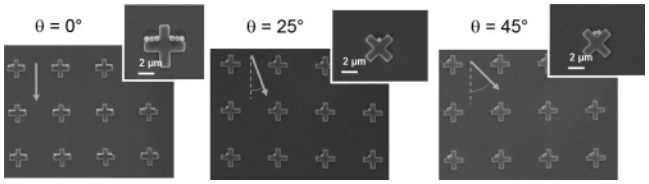

Figure 11. SEM images of 500-nm PS particles placed by capillary assembly in 200-nm-deep cross-shaped patterns on a PDMS substrate using three different pattern orientations (0°, 25°, and 45°) with respect to the motion of the receding meniscus. The assembly was performed with a 0.5% solid content colloidal suspension at a constant withdrawing velocity $v_s = 1$ μm s^{-1} and at a temperature $T_s =$ 25 °C.

patterns on a PDMS substrate using different pattern orientations with respect to the receding meniscus. The assembly was performed with 500-nm PS nanoparticles (0.5% solid content) at a constant substrate velocity of 1 μm s^{-1} and at a constant temperature of 25 °C. Changing the orientation of the structure with respect to the motion of the contact-line direction influences the pinning of the meniscus. This effect can be used to tune the number and the position of particles.

Finally, we also investigated the capability of capillary assembly to create 3D arrangements of particles. We could demonstrate the assembly of 500-nm PS particles in 1.5-μm-deep and 4-μm-wide PDMS patterns. The assembly was performed at a substrate temperature $T_s = 28$ °C and a constant velocity $v_s = 5$ μm s^{-1} with a 1% solid content suspension. While the contact line was being dragged over the template, the geometry of the patterns induced pinning of the suspension in the recessed areas that were filled with particles, whereas no deposition occurred in the surrounding areas. Note that the large depletion of region III induced by the filling of the 3D structures has to be compensated by an appropriate increase in the substrate temperature and in the solid content of the suspension.

5. Conclusions

This study demonstrates that capillary forces and convective flows can be exploited on flat or patterned surfaces to extend the range of structures achievable from single particle placement to almost any 2D arrangements and even some 3D structures. The control of three experimental parameters, namely, the substrate temperature, the contact angle, and the particle concentration, provides full control of the process speed and yield, and allows one to switch between the different assembly regimes. In the two processes investigated, we found that controlling the hydrodynamic flows created by evaporation was critical and that this control can easily be achieved by adjusting the substrate temperature. In convective assembly, the temperature allows rapid and accurate control of the deposition speed, including reversal of the assembly process, whereas, in capillary assembly, a distinct temperature threshold was found that triggered the assembly. This work also demonstrated a threshold in the contact angle of the colloidal suspension. A maximum contact angle value of approximately 65 °C was found to allow capillary assembly, whereas, for lower contact angles (around 15°), a transition from capillary to convective assembly was observed.

The flexibility and compatibility of convective and capillary assembly with a wide range of particle materials and sizes allows one to increase both the structural and functional complexity for novel integrated applications. Beyond patterning applications in which particles, for instance, PS particles, could be used as a resist for pattern transfer, these methods offer the opportunity to build complex devices exploiting either the intrinsic material and surface properties of particles or the more specific properties appearing in well-ordered particle arrangements. For example, storage devices and media could be built using particles as memory cells that could be assembled into well-ordered 2D lattices. Other applications in optics or electronics could benefit from the creation of closely packed metallic particle arrangements to fabricate particle transistors, sensors, or even plasmon-guiding structures that would rely on the coupling effects between regularly spaced particles. Another promising field of application is biology. The capability of combining the unique optical, electronic, or catalytical properties of such structures with the recognition and reactivity functions of biomolecules renders nanoparticles very attractive as building blocks for detection and analysis purposes through novel high-sensitivity nanosensors or high-density bioarrays.[2,38,39] Many of the applications listed above require particles with diameters in the sub-100-nm regime. Both convective and capillary assembly appear to be well-suited for sub-micron-sized particles. However, although the compatibility of comparable approaches has been reported for particle diameters down to 2 nm,[20] the validity of the model we proposed still has to be confirmed for colloids with sizes below 100 nm. Modeling the colloidal assembly process taking into account particle diffusion and hydrodynamics might further complement these studies.

Acknowledgment. The authors thank Ulrich Plachetka at AMO GmbH for providing a high-resolution stamp master. The partial support of the State Secretariat for Education and Research (SER) in the framework of the EC-funded project NaPa (Contract No. NMP4-CT-2003-500120) is gratefully acknowledged. The content of this work is the sole responsibility of the authors. The authors thank Richard Stutz for his assistance in microfabrication, and Walter Riess and Paul Seidler for their continuous support.

LA700852C

(38) Katz, E.; Willner, I. *Angew. Chem.* **2004**, *43*, 6042.
(39) Parak, W. J.; Gerion, D.; Pellegrino, T.; Zanchet, D.; Micheel, C.; Williams, S. C.; Boudreau, M. A.; Le Gros, R.; Larabell, C. A.; Alivisatos, A. P. *Nanotechnology* **2003**, *14*, 15.